

ORIGINAL ARTICLE

Correlation of nuclear morphometry of primary melanoma of the skin with clinicopathological parameters and expression of tumor suppressor proteins (p53 and p16^{INK4a}) and bcl-2 oncoprotein

Z. Mijovic¹, M. Kostov², D. Mihailovic¹, N. Zivkovic¹, M. Stojanovic³, M. Zdravkovic⁴

¹Institute of Pathology, Faculty of Medicine, University of Nis, Nis; ²Department of Pathology, Military Hospital of Nis, Nis; ³Clinic for Surgery, Faculty of Medicine, University of Nis, Nis; ⁴Institute for Forensic Medicine of Nis, Nis, Serbia

Summary

Purpose: To determine the correlation of nuclear morphometry of primary cutaneous malignant melanoma (CMM) with clinicopathological parameters and the expression of p53, p16^{INK4a}, and bcl-2.

Methods: Image analysis and computerized nuclear morphometry were used in a series of 53 primary CMM (nodular melanoma/NM, N=33, and superficially spreading melanoma/SSM, N=20). The clinicopathological parameters determined for each tumor were histological type, maximal tumor diameter, Breslow thickness, Clark level, ulceration, mitotic index (MI) and pathological disease stage. Measured nuclear features included size, shape and optical density (OD). The results were correlated with the expression of p53, p16^{INK4a} and bcl-2.

Results: Significant differences between NM and SSM were found for the nuclear area, OD, and perimeter ($p < 0.05$). MI showed significant correlations with nuclear area, perim-

eter and Feret diameter ($p < 0.05$). In relation to the Clark level, significant differences were found for OD ($p < 0.01$) and circularity of nuclei ($p < 0.05$) between levels II and IV, while the Breslow thickness was not significantly correlated with nuclear morphometric variables. Significantly negative correlations were observed between OD and the expression of p53 and bcl-2, while significant positive correlation was found between the nuclear circularity and p53 immunoreaction intensity. There was no significant correlation between the expression of p16^{INK4a} protein and karyometric variables.

Conclusion: OD and circularity are SIGNIFICANTLY correlated with p53 and bcl-2, and nuclear area with MI. These karyometric variables may determine a more aggressive phenotype of melanoma cells.

Key words: bcl-2 oncoprotein, melanoma, nuclear morphometry, p53 tumor suppressor protein, p16^{INK4a} tumor suppressor protein, skin

Introduction

CMM is a tumor arising from the melanocyte system and displays high malignant potential [1,2]. Melanoma is not an exception in the tumor biology and its occurrence is predominantly the result of accumulation of gene mutations whose key role is the regulation of cellular proliferation, differentiation, apoptosis or some other pathways of cellular death [3,4]. Numerous studies have shown a certain amount of damage and loss of function of tumor suppressor proteins p53 and

p16^{INK4a} and bcl-2 oncoprotein in CMM [5-10].

Nuclear morphometry (karyometry) provides an objective measurement of nuclei using digital imaging and specialized computer software. Nuclear morphometry in an accurate and useful method in the diagnosis and prognosis of various tumors [11-14], including CMM [15-18]. Frequently tested nuclear morphometric variables that best discriminate between benign and malignant lesions are nuclear area, perimeter and nuclear OD [15,16].

The aim of this study was to determine the correlation of nuclear morphometry with clinicopathological parameters, and the expression of p53 and p16^{INK4a} tumor suppressor proteins and bcl-2 oncoprotein of primary CMM.

Methods

Estimation of basic clinicopathological parameters

The study involved 53 samples FROM 53 PATIENTS with primary CMM. There were two histological types: NM detected in 33 patients (62.3%), and SSM detected in 20 patients (37.7%). All tumors were surgically removed by excisional biopsy. For histologic analysis, tissue samples were fixed in 10% buffered formalin, embedded in paraffin wax, sectioned at 5 μ m thick sections and stained with haematoxylin and eosin (H&E). The clinicopathological parameters determined for each tumor were: histological type, tumor size (maximal diameter in cm), tumor thickness in mm (Breslow thickness), tumor invasion (Clark level), ulceration, MI and pathological disease stage. Breslow thickness was determined by ocular micrometer. Clark level of invasion was divided into 5 stages: I - invasion to the epidermis (melanoma *in situ*); II - invasion into the papillary dermis; III - tumor fills the papillary dermis and expands on the papillary-reticular borders; IV - invasion into the reticular dermis; and V - invasion into the subcutaneous adipose tissue. MI was determined in tumor areas with the highest number of mitotic figures per 10 high power microscopic fields (HPF, objective x40) per sample. MI was determined as low MI (1-6 mitotic figures/10 HPF), and high MI (>6 mitotic figures/10 HPF). The pathological tumor stage (pT) was determined according to the classification of the American Joint Committee on Cancer (AJCC-TNM, 2009).

Immunohistochemistry

The study involved 53 samples FROM 53 PATIENTS with primary CMM. There were two histological types: NM detected in 33 patients (62.3%), and SSM detected in 20 patients (37.7%). All tumors were surgically removed by excisional biopsy. For histologic analysis, tissue samples were fixed in 10% buffered formalin, embedded in paraffin wax, sectioned at 5 μ m thick sections and stained with haematoxylin and eosin (H&E). The clinicopathological parameters determined for each tumor were: histological type, tumor size (maximal diameter in cm), tumor thickness in mm (Breslow thickness), tumor invasion (Clark level), ulceration, MI and pathological disease stage. Breslow thickness was determined by ocular micrometer. Clark level of invasion was divided into 5 stages: I - invasion to the epidermis (melanoma *in situ*); II - invasion into the papillary dermis; III - tumor fills the papillary dermis and expands on the papillary-reticular borders;

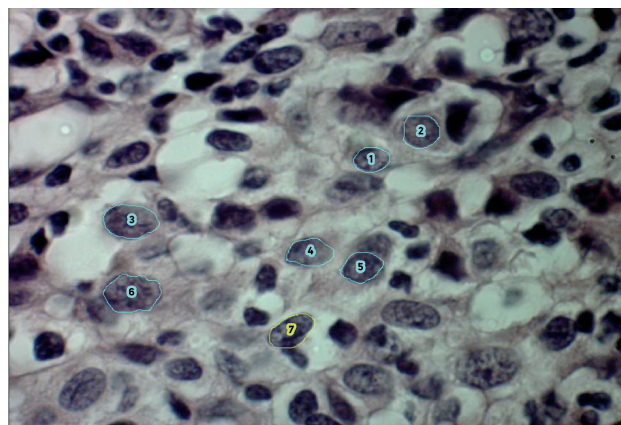


Figure 1. Image analysis of cutaneous malignant melanoma: manual selection of tumor cell nuclei.

IV - invasion into the reticular dermis; and V - invasion into the subcutaneous adipose tissue. MI was determined in tumor areas with the highest number of mitotic figures per 10 high power microscopic fields (HPF, objective x40) per sample. MI was determined as low MI (1-6 mitotic figures/10 HPF), and high MI (>6 mitotic figures/10 HPF). The pathological tumor stage (pT) was determined according to the classification of the American Joint Committee on Cancer (AJCC-TNM, 2009).

Image analysis

Nuclear morphometry was performed on representative H&E stained slides, using Leica DM1000 microscope (Wetzlar, Germany), equipped with a microscopic digital camera Leica EC3 (Germany) connected to a PC (Intel processor, 2.8 GHz, 1GB RAM). Digital microscopic images were obtained using x40 objective lens (NA= 0.65; N plan) and Leica V LAZ EC 1.8.0 imaging software. Microscopic images were obtained in JPEG format and resolution in all cases was 1024x768 pixels. Image segmentation, identification of nuclear contours and nuclear morphometry were performed using Image J version 1.4.367 software (Figure 1). In each case 100 nuclei were measured. The original color micrographs were converted into grayscale images. For each nucleus, the following morphometric parameters were analyzed: nuclear area (area), OD, standard deviation of OD (SD OD), mode value of OD (mode OD), minimal value of OD (min OD), maximal value of OD (max OD), perimeter (perimet), circularity (circular), Feret's diameter (Feret) and Integrated OD (IOD). Nuclear area was defined as the number of pixels. OD was the amount of light that passed through the object: $OD(x,y) = -\log(\text{intensity}(x,y) - \text{black})/(\text{incident light} - \text{black})$. Perimeter was derived from 4 projections in the directions 0°, 45°, 90° and 135°. Circularity was a derived shape measure, calculated from the area and perimeter: $\text{circularity} = 4\pi(\text{area}/\text{perimeter}^2)$. Feret's diameter was the average distance between any two points on the contour of the nucleus. IOD was the sum of individual OD of each pixel in the area being measured. This is equivalent to the product of area and mean gray value.

Table 1. Mean values \pm SD of karyometric variables of cutaneous malignant melanoma

Tumor type	Area (μm^2)	Mean OD	SD OD	Mode OD	Min OD	Max OD	Perimet (μm)	Circular	IOD
NM	56.29 \pm	0.36 \pm	0.11 \pm	0.37 \pm	0.13 \pm	0.70 \pm	28.09 \pm	0.87 \pm	20.24 \pm
	13.25	0.07	0.04	0.08	0.04	0.24	3.54	0.03	6.22
SSM	47.37 \pm	0.43 \pm	0.11 \pm	0.46 \pm	0.16 \pm	0.73 \pm	26.19 \pm	0.85 \pm	20.04 \pm
	10.05	0.08	0.04	0.11	0.05	0.20	3.07	0.05	4.85
p-value	0.01*	0.01*	0.59	0.00*	0.02*	0.85	0.02*	0.08	0.63

* statistically significant differences ($p < 0.05$)

NM: nodular melanoma, SSM: superficially spreading melanoma, Area: nuclear area, Mean OD: mean value of optical density, SD OD: standard deviation of optical density, Mode OD: mode value of optical density, Min OD: minimal value of optical density, Max OD: maximal value of optical density, Perimet: perimeter, Circular: circularity, Feret: Feret's diameter, IOD: integrated optical density

Statistics

The results were statistically analyzed using descriptive and analytical statistical methods: Student's t-test, MANOVA and Pearson's correlation test. A p value less than 0.05 was considered to indicate statistical significance.

Results

Clinicopathological parameters

The mean value of maximal diameter of CMM was 1.6 cm (range 0.3-4). The mean tumor thickness was 4.53 mm (range 0.47-18.9). Clark level III was the most common, found in 20 (37.7%) of the cases. Ulceration was observed in 30 cases (56.6%). MI was high in 37 (69.81%) cases. The most common pathological disease stage was stage IV, found in 23 (43.4%) patients.

Nuclear morphometric features and clinicopathological parameters

Mean values of karyometric variables of the examined histological tumor types are shown in Table 1. Statistically significant differences between NM and SSM were found for the following nuclear morphometric variables: nuclear

area, mean, mode and minimal OD, and perimeter ($p < 0.05$).

Statistically significant correlations were found between MI and the nuclear area ($r = 0.31$), perimeter ($r = 0.30$) and Feret diameter ($r = 0.28$) of CMM ($p < 0.05$).

No significant differences were seen between the nuclear morphometric variables and other clinicopathological parameters.

No statistically significant correlations between Breslow thickness and karyometric variables were found ($p = 0.15$).

MANOVA test showed a statistically significant differences only between Clark levels II and IV (Wilks' lambda=0.31, $F = 3.34$, $p = 0.012$). Statistically significant differences were found for mean and mode value of OD ($p < 0.01$) and circularity of nuclei ($p < 0.05$) between Clark levels II and IV. Clark level II showed the highest mean OD (0.47 ± 0.03), and level IV the lowest (0.36 ± 0.02) (Figure 2). The highest mode value of OD was registered in Clark II level (0.51 ± 0.03), while the lowest value was noted in Clark IV level (0.37 ± 0.02). The highest value of nuclear circularity was found in Clark IV level (0.88 ± 0.01), and the lowest in Clark II level (0.83 ± 0.01) (Figure 3).

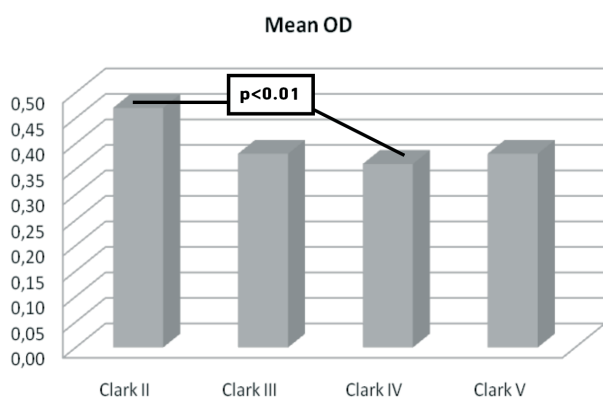


Figure 2. Mean values of optical density (OD) in relation to Clark level of invasion.

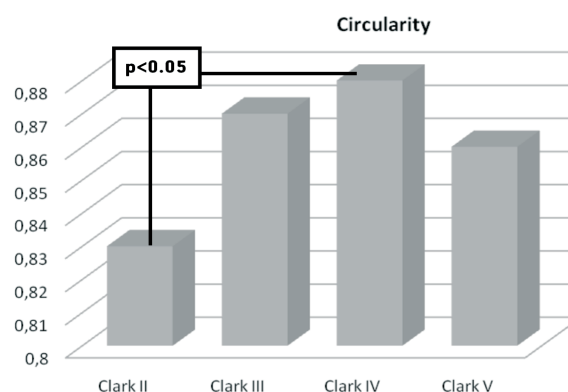


Figure 3. Nuclear circularity in relation to Clark level of invasion.

Table 2. Correlation analysis between the expression of p53, p16^{INK4a} and bcl-2 and karyometric variables of cutaneous malignant melanoma

	Area (μm^2)	Mean OD	SD OD	Mode OD	Min OD	Max OD	Perimet (μm)	Circular	Feret	IOD
P53(%)	0.18	-0.37*	-0.05	-0.39*	-0.32	-0.08	0.14	0.13	0.06	-0.14
P53 int	0.15	-0.35	-0.05	-0.36*	-0.27	-0.10	0.07	0.30*	-0.02	-0.16
Bcl-2(%)	0.16	-0.34*	-0.10	-0.33*	-0.29*	-0.18	0.15	-0.07	0.13	-0.13
Bcl-2 int	0.12	-0.35*	-0.10	-0.35*	-0.33*	-0.15	0.11	-0.12	0.10	-0.17
P16(%)	-0.05	0.17	0.07	0.14	0.05	0.06	0.01	-0.23	0.04	0.06
P16 int	-0.01	0.09	-0.01	0.06	0.04	-0.01	0.04	-0.22	0.07	0.04

* statistically significant correlation ($p < 0.05$)

p53 int: intensity of immunohistochemical expression of p53, Bcl-2 int: intensity of immunohistochemical expression of Bcl-2, P16 int: intensity of immunohistochemical expression of P16. For the rest of the abbreviations see footnote of Table 1

Nuclear morphometric features and expression of tumor suppressor proteins p53 and p16^{INK4a} and bcl-2 oncoprotein

The p53 protein expression was found in 46 (86.8%), p16^{INK4a} protein expression in 25 (47.2%) and bcl-2 oncoprotein expression in 50 (94%) patients.

Statistically significant negative correlations were observed between the percentage of p53 positive cells and p53 intensity of immunoreaction and ODs (mean, mode and minimal ODs). On the other hand, there were statistically significant positive correlations between the p53 immunoreaction intensity and circularity of nuclei.

Statistically significant negative correlations were found between the percentage of bcl-2 positive cells and bcl-2 intensity of immunoreaction and ODs (mean, mode and minimal ODs).

There were no significant correlations between p16 protein expression and karyometric variables (Table 2).

Discussion

Numerous studies have dealt with the diagnostic significance of nuclear morphometry in the evaluation of pigmented skin lesions [15-17,19,20]. A previous study of ours [15] has shown that benign and malignant melanocytic lesions have characteristic features of nuclear morphology and IOD [15]. Karyometric differences between benign and malignant melanocytic lesions reflect alterations at the genetic and epigenetic level during the progression from common melanocytic nevi to dysplastic nevi to melanoma. This process involves dynamic changes in the genome produced by mutations through gain of oncogene function or loss of action of tumor suppressor genes [21]. CMM is a good example of multifactorial disease, for which responsible are both environmental and host factors [2-4]. Loss of

p16 tumor suppressor gene function and mutation of p53 tumor suppressor gene in CMM indicate their role in the pathogenesis of this malignancy [7,22]. High level of bcl-2 oncoprotein expression was detected in 90% of malignant melanomas and benign melanocytic tumors, indicating that bcl-2 oncoprotein overexpression is not a key event in the malignant transformation of melanocytes [23].

The use of computerized image analysis has contributed to an objective description of melanoma cells. Bedin et al. [24] reported that the nuclear area is a significant unfavorable prognostic factor along with increasing tumor thickness, i.e. vertical growth, nuclear area enlarged and nuclei tending to loose their roundness. Talve et al. [19] have shown that the nuclear area, and the short and long axis of nuclei correlated with the thickness of melanoma, but the axis ratio of nuclei (which reflects the circularity of the nuclei) and the melanoma thickness were not correlated to each other. The results of another study showed that the thickness of melanoma correlates with nuclear size in aneuploid, but not in diploid melanomas. The frequency of aneuploidy was not increased with tumor thickness [25]. In our investigation, no significant correlation between Breslow thickness and the karyometric variables was found. However, melanoma cells in the deeper part of the tumors frequently exhibit greater nuclear heterogeneity in the appearance and size of the nuclei. On the other hand, we found statistically significant differences between the two histological types of CMM (nodular and superficially spreading melanoma) for the nuclear area, OD, and perimeter. Higher values of these variables in nodular melanoma are in line with the biological potential of the tumor. The presence of vertical growth phase in melanoma increases the capacity of developing metastases [26,27].

In our study MI showed correlations with the nuclear area, perimeter and Feret's diameter. These

karyometric results support the findings of Talve et al. [28], suggesting that tumors with high MI tend to have rounder and larger nuclei. Thus the size and form of tumor cell nuclei may indirectly reflect their proliferative activity.

p53 gene plays a role in programmed cell death by decreasing the expression of bcl-2 and increasing that of bax. p53 induces apoptosis in response to genotoxic stimuli and maintains genomic stability. Loss of these functions, either through mutations or by allelic deletion, leads to enhanced genomic instability, gene amplification and changes in DNA ploidy [29]. The characteristics of the nuclear architecture, as seen by the pathologist in routine sections, reflect genomic and non-genomic changes in both the DNA structure and chromatin [30]. Our study showed a statistically significant negative correlation between the expression p53 protein and bcl-2 oncoprotein (in the percentage of positive cells and immunoreaction intensity) and OD. IOD takes into account chromosome copy number, extra chromosomal fragments and the DNA content of individual chromosomes, as well as morphometric nuclear features [31]. Talve et al. [28] showed that p53 positive nuclei of CMM had a larger mean nuclear area than p53 negative ones. They did not examine the nuclear OD, but in their research MI showed a positive correlation with the nuclear area, similarly with our results. Furthermore, MI was highest in the group with highest p53 positivity.

In relation to Clark level, we found significant differences in OD and circularity of nuclei between levels II and IV, while Breslow thickness was not significantly correlated with nuclear morphometric variables. Melanomas with lower values of OD and higher circularity of nuclei had a higher Clark level. Our results are partially consistent with the findings of Karbowniczek et al. [18] who found that with growing thickness according to Breslow and increased Clark level, the mean nuclear area of tumor cells increased, and their shape became more round. On the other hand, in this study, the MIB-1 posi-

tive tumor cell nuclei of primary melanomas with metastases were less round in comparison to primary melanomas without metastases. These findings indicate an association between the area and shape of melanoma cell nuclei and the presence of metastases, and between the nuclear area of tumor cells and factors related to poor prognosis, such as the depth of invasion and the tumor thickness [18]. Indeed, melanomas with Clark I and II levels have a lower potential for disease progression and are virtually always curable with complete local excision. Most of Clark level II melanomas are not tumorigenic, with radial phase of growth. Higher levels of invasion (Clark III, IV and V) have a higher metastatic potential [26,27].

In our previous immunohistochemical investigation [32] significant correlations between p53 overexpression, Breslow thickness and Clark level were found; bcl-2 oncoprotein overexpression was correlated only with Breslow thickness, while no correlation with the p16 tumor suppressor protein expression was detected. Therefore, these evaluated proteins may be markers of aggressive biological tumor activity. In the study of Ilmonen et al. [7], p53 and bcl-2 expression of primary melanomas showed no association with tumor thickness or tumor invasion level, but strong p53 and bcl-2 immunoreactivity were associated with adverse prognosis [7].

In the available literature, no data of morphometric evaluation of melanoma in relation to the expression of p16 and bcl-2 were found. In our study, no correlation between the expression of p16 protein and the examined nuclear variables was found.

Conclusion

CMM with lower value of nuclear OD and higher circularity of nuclei had a higher level of Clark invasion. OD and circularity were correlated with p53 and bcl-2 expression, and nuclear area with MI. These karyometric variables may imply more aggressive phenotype of melanoma cells.

References

1. Barnhill RL. Malignant melanoma. In: Barnhill RL, Piepkorn Busam KJ (Eds): Pathology of melanocytic nevi and malignant melanoma (2nd Edn). Springer Science, New York, 2004, pp 238-356.
2. Boyle P, Levin B. World Cancer Report 2008. Cutaneous melanoma. IARC Press, Lyon, 2008.
3. Carlson JA, Ross JS, Slominski AJ et al. Molecular diagnostics in melanoma. *J Am Acad Dermatol* 2005; 52: 743-775.
4. Crowson AN, Magro C, Miller A, Mihm MC Jr. The molecular basis of melanomagenesis and the metastatic phenotype. *Semin Oncol* 2007; 34: 476-490.
5. Stefanaki C, Stefanaki K, Antoniou C et al. G1 cell cy-

- cle regulators in congenital melanocytic nevi. Comparison with acquired nevi and melanomas. *J Cutan Pathol* 2008; 35: 799-808.
6. Straume O, Akslen LA. Alterations and prognostic significance of p16 and p53 protein expression in subgroups of cutaneous melanoma. *Int J Cancer* 1997; 74: 535-539.
 7. Ilmonen S, Hernberg M, Pyrhonen S, Tarkkanen J, Asko-Seljavaara S. Ki - 67, Bcl - 2 and p53 expression in primary and metastatic melanoma. *Melanoma Res* 2005; 15: 375-381.
 8. Yu H, McDaid R, Lee J et al. The role of BRAF mutation and p53 inactivation during transformation of a subpopulation of primary human melanocytes. *Am J Pathol* 2009; 174: 2367-2377.
 9. Straume O, Sviland L, Akslen LA. Loss of nuclear p16 protein expression correlates with increased tumor cell proliferation (Ki-67) and poor prognosis in patients with vertical growth phase melanoma. *Clin Cancer Res* 2000; 6: 1845-1853.
 10. O'Leary TJ. Skin. In: O'Leary TJ (Ed): *Advanced diagnostic methods in pathology: principles, practice, and protocols* (1st Edn). Saunders, Philadelphia, 2003, pp 459-476.
 11. Abdalla F, Boder J, Markus R, Hashmi H, Buhmeida A, Collan Y. Correlation of nuclear morphometry of breast cancer in histological sections with clinicopathological features and prognosis. *Anticancer Res* 2009; 29: 1771-1776.
 12. Chiusa L, Margaria E, Pich A. Nuclear morphometry in male breast carcinoma: association with cell proliferative activity, oncogene expression, DNA content and prognosis. *Int J Cancer* 2000; 89: 494-499.
 13. Wang S-L, Wu M-T, Yang S-F, Chan H-M, Chai C-Y. Computerized nuclear morphometry in thyroid follicular neoplasms. *Pathol Int* 2005; 55: 703-706.
 14. Mijovic Z. *Morphological and morphometric features of lung carcinoma (monograph)*. School of Medicine, Nis, 2008 (in Serbian).
 15. Mijovic Z, Mihailovic D. Discriminant analysis of image karyometric variables in benign and malignant melanocytic skin lesions. *Analyt Quant Cytol Histol* 2002; 24: 314-316.
 16. Leitinger G, Cerroni L, Soyer HP, Smolle J, Kerl H. Morphometric diagnosis of melanocytic skin tumors. *Am J Dermatopathol* 1990; 12: 441-445.
 17. Li L-XL, Crotty KA, Scolyer RA et al. Use multiple cytometric markers improves discrimination between benign and malignant melanocytic lesions: a study of DNA microdensitometry, karyometry, argyrophilic staining of nucleolar organizer regions and MIB1-Ki67 immunoreactivity. *Melanoma Res* 2003; 13: 581-586.
 18. Karbowniczek M, Chosia M, Domagala W. Nuclear morphometry of MIB-1 positive and negative tumor cells in primary and metastatic malignant melanoma of the skin. *Pol J Pathol* 1999; 50: 235-241.
 19. Talve LA, Collan YU, Ekfors TO. Nuclear morphometry, immunohistochemical staining with Ki-67 antibody and mitotic index in the assessment of proliferative activity and prognosis of primary malignant melanomas of the skin. *J Cutan Pathol* 1996; 23: 335-343.
 20. Mauri MF, Boi S, Miccolo R, Cristofolini M, Dalla Palma P. Morphometric analysis in prognostic evaluation of stage I thick cutaneous melanomas. *Anal Quant Cytol Histol* 1997; 19: 311-315.
 21. Carlson JA, Ross JS, Slominski AJ. New techniques in dermatopathology that help to diagnose and prognosticate melanoma. *Clin Dermatol* 2009; 27:75-102.
 22. Sekulic A, Haluska PJr, Miller AJ et al. Malignant melanoma in 21st century: the emerging molecular landscape. *Mayo Clin Proc* 2008; 83: 825-846.
 23. Cerroni L, Soyer HP, Kerl H. Bcl-2 protein expression in cutaneous malignant melanoma and benign melanocytic nevi. *Am J Dermatopathol* 1995; 17: 7-11.
 24. Bedin V, Adam RL, Sa B, Landman G, Metze K. RFractal dimension of chromatin is an independent prognostic factor for survival in melanoma. *BMC Cancer* 2010; 10:260. <http://www.biomedcentral.com/1471-2407/10/260>.
 25. Talve LA, Collan YU, Ekfors TO. Primary malignant melanoma of the skin. Relationships of nuclear DNA content, nuclear morphometric variables, Clark level and tumor thickness. *Analyt Quant Cytol Histol* 1997; 19: 62-74.
 26. Crowson AN, Magro CM, Mihm MC Jr. Prognosticators of melanoma, the melanoma report, and the sentinel lymph node. *Mod Pathol* 2006; 19: 71-87.
 27. Elder DE, Thompson JF, Barnhill RL et al. Melanocytic tumours. In: LeBoit PE, Burg G, Weedon D, Sarasain A (Eds): *World Health Organization Classification of Tumours. Pathology and Genetics of Skin Tumours*. IARC Press, Lyon, 2006, pp 50-102.
 28. Talve L, Kainu J, Collan Y, Ekfors T. Immunohistochemical expression of p53 protein, mitotic index and nuclear morphometry in primary malignant melanoma of the skin. *Pathol Res Pract* 1996; 192: 825-833.
 29. Hussein MR, Haemel AK, Wood GS. p53-related pathways and the molecular pathogenesis of melanoma. *Eur J Cancer Prev* 2003; 12: 93-100.
 30. Rothhammer T, Bosserhoff AK. Epigenetic events in malignant melanoma. *Pigment Cell Res* 2007;20: 92-111.
 31. Huang Q, Yu C, Klein M, Fang J, Goyal RK. DNA index determination with automated cellular imaging system (ACIS) in Barrett's esophagus: comparison with CAS 200. *BMC Clin Pathol* 2005; 5:7. doi:10.1186/1472-6890-5-7.
 32. Kostov M, Mijovic Z, Mihailovic D, Cerovic S, Stojanovic M, Jelic M. Correlation of cell cycle regulatory proteins (p53 and p16^{ink4a}) and bcl-2 oncoprotein with mitotic index and thickness of primary cutaneous malignant melanoma. *Bosn J Basic Med Sci* 2010; 10: 276-281.